

Study of differentially expressed genes related to plant height and yield in two alfalfa cultivars based on RNA-seq

Jiangjiao Qi¹, Xue Yu¹, Xuzhe Wang¹, Fanfan Zhang¹, Chunhui Ma^{Corresp. 1}

¹ College of Animal Science & Technology, Shihezi University, Shihezi, Xinjiang, China

Corresponding Author: Chunhui Ma
Email address: chunhuima@126.com

Background. Alfalfa (*Medicago sativa* L.) is a kind of forage with high relative feeding value in farming and livestock breeding, and is of great significance to the development of animal husbandry. The growth of the aboveground part of alfalfa is an important factor that limits crop yield. Clarifying the molecular mechanisms that maintain vigorous growth in alfalfa may contribute to the development of molecular breeding for this crop.

Methods. Here, we evaluated the growth phenotypes of five cultivars of alfalfa (WL 712, WL 525HQ, Victoria, Knight 2, and Aohan). Then RNA-seq was performed on the stems of WL 712, chosen as a fast growing cultivar, and Aohan, chosen as a slow growing cultivar. GO enrichment analysis was conducted on all differentially expressed genes (DEGs).

Result. Among the differentially expressed genes that were up-regulated in the fast growing cultivar, GO analysis revealed enrichment in the following seven categories: formation of water-conducting tissue in vascular plants, biosynthesis and degradation of lignin, formation of the primary or secondary cell wall, cell enlargement and plant growth, cell division and shoot initiation, stem growth and induced germination, and cell elongation. KEGG analysis showed that differentially expressed genes were annotated as being involved in plant hormone signal transduction, photosynthesis, and phenylpropanoid biosynthesis. KEGG analysis also showed that up-regulated in the fast growing cultivar were members of the *WRKY* family of transcription factors related to plant growth and development, members of the *NAC* and *MYB* gene families related to the synthesis of cellulose and hemicellulose, and the development of secondary cell wall fibres, and finally, *MYB* family members that are involved in plant growth regulation. Our research results not only enrich the transcriptome database of alfalfa, but also provide valuable information for explaining the molecular mechanism of fast growth, and can provide reference for the production of alfalfa.

1 ~~Study of differentially expressed genes related to plant height and yield in two alfalfa~~
2 ~~cultivars based on RNA-seq~~

3
4 Jiangjiao Qi, Yuxue, Xuzhe Wang, Fanfan Zhang and Chunhui Ma

5 College of Animal Science & Technology, Shihezi University, Shihezi, 832003, Xinjiang, China

6 Corresponding Author:

7 Chunhui Ma

8 Shihezi University, Shihezi, 832003, Xinjiang, China

9 E-mails: chunhuima@126.com

10 **Abstract**

11 **Background.** Alfalfa (*Medicago sativa* L.) is a kind of forage with high relative feeding
12 value in farming and livestock breeding, and is of great significance to the development of
13 animal husbandry. The growth of the aboveground part of alfalfa is an important factor that
14 limits crop yield. Clarifying the molecular mechanisms that maintain vigorous growth in alfalfa
15 may contribute to the development of molecular breeding for this crop.

16 **Methods.** Here, we evaluated the growth phenotypes of five cultivars of alfalfa (WL 712,
17 WL 525HQ, Victoria, Knight 2, and Aohan). Then RNA-seq was performed on the stems of
18 WL 712, chosen as a fast growing cultivar, and Aohan, chosen as a slow growing cultivar. GO
19 enrichment analysis was conducted on all differentially expressed genes (DEGs).

20 **Result.** Among the differentially expressed genes that were up-regulated in the fast
21 growing cultivar, GO analysis revealed enrichment in the following seven categories: formation
22 of water-conducting tissue in vascular plants, biosynthesis and degradation of lignin, formation
23 of the primary or secondary cell wall, cell enlargement and plant growth, cell division and shoot
24 initiation, stem growth and induced germination, and cell elongation. KEGG analysis showed
25 that differentially expressed genes were annotated as being involved in plant hormone signal
26 transduction, photosynthesis, and phenylpropanoid biosynthesis. KEGG analysis also showed
27 that up-regulated in the fast growing cultivar were members of the *WRKY* family of
28 transcription factors related to plant growth and development, members of the *NAC* and *MYB*
29 gene families related to the synthesis of cellulose and hemicellulose, and the development of
30 secondary cell wall fibres, and finally, *MYB* family members that are involved in plant growth
31 regulation. Our research results not only enrich the transcriptome database of alfalfa, but also
32 provide valuable information for explaining the molecular mechanism of fast growth, and can
33 provide reference for the production of alfalfa.

34
35 **Key words:** *Medicago sativa*, RNA-seq, DEGs, Stem elongation, Fast growing, Slow growing

42 Introduction

43 The stem is an important vegetative organ between the root and leaf of a plant and
44 transports nutrients and water (Ernest et al., 2020). The stems of alfalfa also play a role in
45 photosynthesis, nutrient storage, and regeneration (Pablo & Miguel, 2018). In the process of
46 stem growth and development, stem tips grow continuously, whereas branches, leaves, and
47 lateral branches are produced successively, which together constitute a huge branch system (Yu
48 et al., 2015; Jaykumar & Mahendra, 2016). The degree of stem development is closely related
49 to the life cycle of plants (Sophia et al., 2021), especially the aboveground biomass of the plant
50 (Kleyer et al., 2019). Alfalfa, with stems and branches as the main components of biomass yield,
51 is a typical representative crop.

52 Alfalfa is a feed crop with a high economic value (Kumar et al., 2018). In addition to its
53 stress resistance properties, it has been the focus of research because of its perennial nature and
54 high nutritional value (Wang et al., 2017; Diatta, Doohong & Jagadish, 2021). The stems and
55 leaves of alfalfa have a high nutrient content and are the main parts areas of animal forage (Sulc
56 et al., 2021). Owing to the cross-pollination of alfalfa, most cultivars have a complex genetic
57 background. Restricted by its genetic characteristics, growth performance and nutritional
58 quality are uneven (Bambang et al., 2021). Alfalfa stalks are composed of nodes and internodes,
59 which affect plant height and yield. The height and stem diameter of alfalfa are important
60 factors that restrict its biomass (Monirifar, 2011). Therefore, increasing the number of alfalfa
61 vegetative branches, vegetative growth time, and delaying the flowering time of plants are
62 crucial for improving the nutritional quality and yield of forage grass (Aung et al., 2015).

63 Previous studies have reported significant differences in alfalfa plant height and biomass
64 yield among cultivars (Ziliotto et al., 2010). The series of WL alfalfa cultivars had the best
65 growth performance when compared among cultivars (Tetteh & Bonsu, 1997). Plant spacing
66 and light significantly effect alfalfa forage yield and weed inhibition (Celebi et al., 2010).
67 Compound fertilizers can increase the nutrient content of soil and improve the yield of alfalfa
68 (Iryna, Rudra & Doohong, 2021; Na et al., 2021). Additionally, the growth and development
69 periods of alfalfa are equally important for its yield (Martin et al., 2010). During the growth of
70 alfalfa, the budding stage, which has excellent nutritional quality and biomass yield, has always
71 been a period of concern for breeders (Fan et al., 2018). Currently, research on the growth
72 performance of alfalfa mainly focuses on the physiological level. Few reports have revealed the
73 molecular mechanism of alfalfa stem elongation and diameter enlargement.

74 Owing to the lack of a complete reference genome sequence, previous studies on the stress-
75 response genes of alfalfa have used nonparametric transcriptome analysis (Yuan et al., 2020;
76 Wang et al., 2021; Gao et al., 2016; Arshad, Gruber & Hannoufa et al., 2018). Reference-free
77 transcriptome refers to the sequencing of eukaryotic transcriptomes in the absence of a
78 reference genome. After obtaining the original data for eukaryotic nonparametric transcriptome
79 sequencing, the quality control splicing is first performed to generate unigenes, which are then
80 used as the reference sequence for subsequent analysis. However, with the availability of whole-
81 genome sequencing and annotation of alfalfa (Zhongmu 1), studying the alfalfa genome has
82 become easier (Zhang et al., 2021).

83 Transcriptome sequencing is the study of all mRNAs present in a given sample, which is
84 the basis for the study of gene function and is important for understanding the development of

85 organisms. With the advantages of high-throughput, high accuracy, and high sensitivity, RNA-
86 seq can be used to study changes in the expression level of transcripts to understand or reveal
87 the intrinsic relationship between gene expression and biological phenotypes. At present, RNA-
88 seq technology has become a common method to study the growth and development of many
89 plants (Chen et al., 2020; Kim et al., 2021; Zheng et al., 2021). Next-generation high-throughput
90 sequencing technology can be used to comprehensively obtain the transcript information of
91 alfalfa and screen out genes related specifically to stem elongation and diameter enlargement.

92 The growth rate of alfalfa is an important factor that affects plant height and yield (Yan et
93 al., 2021). Exploring the molecular mechanisms in alfalfa that regulate growth rate may be
94 helpful to improve yield. Here, we identified differentially expressed genes (DEGs) in the stem
95 of alfalfa "WL 712" (USA, Fall Dormancy = 10.2) and "Aohan" (China, Fall Dormancy = 2.0)
96 using RNA-seq. We further identified key genes influencing vigorous-growing alfalfa by
97 bioinformatics analysis and predicted their functions. These results may be helpful in clarifying
98 the molecular mechanism that regulate growth rate in alfalfa, establishing a regulatory network
99 of the growth and development of dominant cultivars, and laying a theoretical foundation for
100 molecular breeding and the introduction of productive cultivars.

102 **Materials & Methods**

103 **Characterisation of phenotypic traits**

104 Five cultivars of alfalfa, *Medicago sativa* L. (WL 712, Victoria, WL 525HQ, Knight 2, and
105 Aohan) were planted at the experimental station of Shihezi University, Xinjiang, China (N44 °
106 20 ', E88 ° 30', altitude 420 m) (**Table S1a**). Its characteristic is temperate continental arid
107 climate, with an average annual temperature of 8.1°C. Before planting, we adopted the "S"
108 shaped sampling method, and nine soil samples were obtained. The nutrient status of the soil
109 (20 cm) was as follows: available nitrogen 92.6 mg/kg, organic matter 12.4 g/kg, available
110 potassium 168.5 mg/kg, available phosphorus 33.2 mg/kg, and pH 7.26 (**Table S1b**).

111 In June 2019 and 2020, alfalfa was planted in a 40 m² plot using a completely randomised
112 design. To ensure consistency among the cultivars, thirty-six stems were collected from a well-
113 growing single plant of each cultivar. The single-row planting method was used with sampling
114 plant spacing of 40 cm and row spacing of 60 cm, with three biological replicates per cultivar.
115 At the budding stage, agronomic traits of five randomly selected plants were determined from
116 each of the three biological replicates. The absolute distance from the root to the top of the main
117 stem was measured as plant height by using a ruler. The number of branches and nodes was
118 counted. The stem diameter and internode length were measured by using calipers. The leaf
119 area was measured by using a leaf area meter. Five plants in each row were randomly selected
120 and weighed, and the average value was calculated as the total fresh weight per plant. By
121 comparing and analyzing the growth indexes of different varieties, it was finally determined
122 that WL 712 represented a vigorous and fast growing variety and Aohan represented a short
123 and slow growing variety (**Fig. 1**).

124 **Cultivation of experimental materials and sample collection**

125 Stems of WL 712 and Aohan were collected and cut into 8 cm pieces, leaving an axillary
126 bud. The stems were cultivated on cutting beds in the greenhouse (light/dark: 16 h / 8 h, Temp:
127 25 °C / 20 °C, humidity 70%) of the Beiyuan campus of Shihezi University for 20 days, and
128 surviving plants were transplanted into plastic pots (diameter 32 cm, height 35 cm). Nutrient

129 soil: vermiculite = 1: 1 (cultivation and management methods were consistent). More than 30
130 individual plants of both WL 712 and Aohan survived in the greenhouse. Five plants each of
131 WL 712 and Aohan alfalfa were randomly selected and the plant height, internode length, stem
132 diameter, leaf area and yield were determined.

133 At the budding stage (about 42 days after transplanting), the plant height of WL 712 and
134 Aohan reached 50.2 cm and 28.7 cm (**Table 1**), respectively. We collected the main stem and
135 removed its top and base. The middle part of the main stem (approximately 1.5 cm in length)
136 of each cultivar was collected, quickly frozen in liquid nitrogen. Three biological replicates
137 were used for per cultivar. WJ1, WJ2 and WJ3 represent samples from the WL 712 cultivar.
138 AJ1, AJ2 and AJ3 represent samples from the Aohan cultivar. Finally, six samples were used
139 for RNA-seq.

140 **Library construction and RNA-seq**

141 Total RNA was isolated from stems using the RNeasy Plant Mini Kit (Qiagen, Germany).
142 A total of 3 μg RNA per sample was used to build the library. Sequencing libraries were
143 generated using a NEBNext Ultra RNA Library Prep Kit (NEB, USA). Messenger RNA was
144 purified from each sample using magnetic beads and fragmented with divalent cations at
145 elevated temperature. First-strand cDNA was obtained using segmented mRNA as template and
146 random oligonucleotide as primer. Then, the second strand of cDNA was obtained in a DNA
147 polymerase I system. The double-stranded cDNA was purified using AMPure XP Beads
148 (Beckman Coulter, Beverly, USA). The double-stranded cDNA was ligated to the sequencing
149 adaptor after terminal repair and A tail, and 250-300 bp cDNA was obtained using AMPure XP
150 beads. Finally, the PCR system was amplified, and the PCR products were purified again using
151 AMPure XP beads to obtain the libraries.

152 Library quality was examined using the Agilent Bioanalyzer 2100 system. The effective
153 concentration of the library (≥ 2 nM) was quantified using qRT-PCR. After passing the
154 inspection, the libraries were pooled and sequenced on the Illumina HiSeq X-10 (California,
155 USA) platform by Beijing Novo Biotech Company, Ltd. Finally, each sample contained an
156 average of 6.63 G of valid data, and 4.42×10^7 clean reads.

157 **Quality control**

158 To ensure the accuracy of data analysis, we filtered the original data and examined the
159 sequencing error rate. Using in-house Perl scripts to process the raw reads of fastq format.
160 Removing reads containing adapters, ploy-N sequences, and low-quality from the raw data to
161 obtain clean reads. The Q_{20} , Q_{30} , and GC contents of the clean data were calculated. All
162 subsequent analyses depend on clean data, high quality.

163 **RNA-seq data analysis**

164 The analysis and calculation of all transcriptome data referred to a previous research report
165 (Trapnell et al., 2012). In brief, the index of the reference genome was constructed using
166 HISAT2 v2.2.1. The paired-end clean reads were obtained using HISAT2 v2.2.1
167 (<https://cloud.biohpc.swmed.edu/index.php/s/fe9QCsX3NH4QwBi/download>) aligned to the
168 reference genome Zhongmu No. 1
169 (https://figshare.com/articles/dataset/genome_fasta_sequence_and_annotation_files/12327602) to
170 obtain mapped reads (Mortazavi, Williams & McCue, 2008). We also analysed the proportion
171 of mapped reads in the exons, introns, and intergenic regions of the genome.

172 The clean reads aligned to Zhongmu No. 1 were quantified using FeatureCounts v1.5.0-

173 p3. Gene expression was represented as FPKM (fragments per kilobase of transcript per million
174 fragments mapped), and differences between WL 712 and Aohan FPKM values were compared
175 using FeatureCounts v1.5.0-p3.

176 Differential expression analysis of the two comparison combinations was performed using
177 the DESeq2 R package (1.16.1)
178 (<https://www.bioconductor.org/packages/release/bioc/html/DESeq2.html>). DESeq2 determines the
179 differential expression in digital gene expression data using a model based on a negative
180 binomial distribution. The corrected P-values and $|\log_2\text{foldchange}|$ are thresholds for significant
181 differential expression. P-values were adjusted using the Benjamini & Hochberg method.

182 Gene Ontology (GO) (<http://www.geneontology.org/>) enrichment and KEGG (Kyoto
183 Encyclopedia of Genes and Genome) (<http://www.genome.jp/kegg/>) statistical analysis of DEGs
184 were performed using the clusterProfiler R package. A corrected P-value less than 0.05 was
185 used as the threshold for significant enrichment of differentially expressed genes.

186 qRT-PCR

187 The accuracy of the RNA-seq was verified by qRT-PCR. Total RNA was isolated from
188 stems, and cDNA was synthesised by using the PrimeScript RT reagent Kit (Takara, Tokyo,
189 Japan). Alfalfa β -Actin 2 was used as the internal reference gene. The primers in **Table S2** were
190 used for qRT-PCR. qRT-PCR was completed using the LightCycler 96/LightCycler480 system.
191 The solution of the 20 μ L system contained 0.4 μ L forward primer, 0.4 μ L reverse primer, 10
192 μ L TB Green Fast qPCR Mix (2X) (Takara, Tokyo, Japan) and 2 ng cDNA. The PCR procedure
193 included 45 cycles, with 3 technical repeats for each reaction. According to Kenneth report,
194 the relative expression of each gene was calculated (Livak & Schmittgen, 2001).

195 Statistical Analysis

196 All statistical analysis was using SPSS software (version 17; IBM Inc, USA). The data
197 were compared using Student's t-test, and $P < 0.05$ was considered statistically significant. The
198 power of our samples was calculated using RNASeqPower
199 (<https://bioconductor.org/packages/release/bioc/html/RNASeqPower.html>), and the RNASeqpower
200 was 94.2%.

201
202
203
204
205
206
207
208
209
210
211
212
213
214
215
216

217 **Results**218 **Phenotypic analysis of five alfalfa varieties**

219 To compare the differences in the growth patterns of the five cultivars (**Table S1a**), plant
220 height, internode length and stem diameter of alfalfa at different growth stages were continually
221 measured in 2019 and 2020 (**Fig. 2, Table S3**). There were no significant differences in plant
222 height, internode length or stem diameter among cultivars at the seedling transplant stage. After
223 the budding stage, plant height, internode length and stem diameter of different alfalfa varieties
224 reached a plateau and remained relatively stable (**Fig. 2a-c**). In 2019 and 2020, WL 712 and
225 Aohan represented tall and short phenotypes, respectively (**Fig. 2d**). Comparing the agronomic
226 traits of alfalfa at the budding stage in 2019 and 2020, the plant height of WL 712 was
227 approximately 1.78 and 1.91 times those of Aohan, respectively, and the stem diameter of WL
228 712 was approximately 1.90 and 1.92 times those of Aohan (**Fig. 2d-e**). The internode length
229 and number of lateral branches in WL 712 were significantly larger than those in Aohan ($P <$
230 0.01), whereas the number of main branches in WL 712 was significantly lower ($P < 0.05$) (**Fig.**
231 **2f, Fig. 3a-b**).

232 To identify the correlation between internode length and stem diameter and other traits,
233 the fresh weight, leaf-stem ratio, and dry weight of the five cultivars were also determined. The
234 results showed that the production performances of WL 712 and Aohan were significantly
235 different ($P < 0.05$) (**Fig. 3c-f**). Phenotypic correlation analysis based on 8 agronomic traits was
236 done. We found that fresh and dry weight were positively and strongly correlated with the
237 number of lateral branches, plant height, stem diameter, and internode length, and plant height
238 was significantly positively correlated with internode length ($P < 0.01$). In addition, the number
239 of main branches was negatively correlated with plant height, stem diameter, and internode
240 length ($P < 0.01$) (**Table 2**).

241 From the screening of five alfalfa cultivars, WL 712 and Aohan were identified as the
242 cultivars with the most significant difference in growth performance (**Fig. 1**). The growth trend
243 of the two varieties in greenhouse is similar to that in field. The plant height, internode length,
244 yield per plant, leaf area and stem diameter of WL 712 alfalfa were significantly higher than
245 those of Aohan alfalfa (**Table 2**).

246 Based on the above results, WL 712 and Aohan were used as the vigorous-growing and
247 slow-growing experimental cultivars. A piece of the stem, midway between stem tip and base,
248 of plants at the budding stage (approximately 42 days after transplanting) was used for RNAseq.
249 **RNA-seq analysis**

250 Using RNA-seq, we obtained 2.74×10^8 raw reads. The sequence error rate of a single
251 base position was 0.03%, and the average GC content was 41.65%. After filtering from the raw
252 data, 2.65×10^8 (96.94%) clean reads (39.76 G) were obtained. The phred values were greater
253 than 97% and 93% at Q_{20} and Q_{30} , respectively (**Table S1c**). The Pearson coefficient showed
254 that the homology among the samples within the group was higher than 84.6% (**Fig. S1**).

255 We aligned the clean reads with the reference genome. The average proportions of exons,
256 introns and intergenic regions in AJ samples were 72.72%, 3.61%, and 23.67%, respectively.
257 Similarly, the WJ samples accounted for 74.14%, 2.96%, and 22.90%, respectively (**Table S4**).
258 The reads aligned to the intron region may have been derived from the precursor mRNA. The
259 reads aligned to the intergenic region may have been derived from ncRNAs.

260 Additionally, according to the comparison of RNA-seq data from WL 712 and Aohan, the

261 RNASeq power of our sample was 94.2%. The result may be beneficial to screen and explore
262 the functional DEGs related to the vigorous-growing of alfalfa. These results demonstrated that
263 the experiments were reproducible and that the data were accurate.

264 **Identification and functional annotation of DEGs in WL 712 and Aohan**

265 Generally, the gene expression value of RNA-seq is evaluated as fragments per kilobase
266 of transcript per million mapped reads (FPKM), which corrects the sequencing depth and gene
267 length (**Fig. S2**). More than 90% of the clean reads were successfully mapped to the alfalfa
268 genome. To clarify the function of the DEGs between WL 712 and Aohan, we performed GO
269 and KEGG enrichment analyses. In total, 954 DEGs were significantly enriched and assigned
270 to 35 GO terms. Compared to Aohan, WL 712 upregulated 578 genes and downregulated 376
271 genes. Among the molecular function, “*protein heterodimerization activity*” [GO:0046982]
272 (114 DEGs, 11.95%) was the highest proportion, followed by “*UDP-glycosyltransferase*
273 *activity*” [GO:0008194] (99 DEGs, 1.04%) and “*translation factor activity, RNA binding*”
274 [GO:0008135] (86 DEGs, 9.01%). Among the cell components, “*bounding membrane of*
275 *organelle*” [Go:0098588] (57 DEGs, 5.97%) represented the largest cluster, followed by “*whole*
276 *membrane*” [Go:0098805] (49 DEGs, 5.13%) and “*peptidase complex*” [Go:1905368] (44
277 DEGs, 4.61%). Among the biological processes, “*translational elongation*” [GO:0006414] (41
278 DEGs, 4.30%) represented the largest cluster (**Table 3, Table S5, Fig. 4**).

279 Based on biological system network, the function of DEG was identified using KEGG
280 classification. A total of 1324 genes were enriched in 110 KEGG pathways (**Fig. 5**). “*Carbon*
281 *metabolism*” [ath01200] (103 DEGs, 7.8%) and “*Ribosome*” [ath03010] (96 DEGs, 7.3%) were
282 the most abundant pathways; followed by “*Biosynthesis of amino acids*” [ath01230] (81 DEGs,
283 6.1%), “*RNA transport*” [ath03013] (54 DEGs, 4.1%), “*Plant-pathogen interaction*” [ath04626]
284 (52 DEGs, 3.9%), “*Protein processing in endoplasmic reticulum*” [ath04141] (52 DEGs, 3.9%)
285 and “*Plant hormone signal transduction*” [ath04075] (44 DEGs, 3.2%) (**Table S6**).

286 **Expression and regulation of DEGs in WL 712 and Aohan**

287 KEGG analysis showed that DEGs related to stem elongation and diameter enlargement
288 were widely involved in biological processes such as hormone signalling, photosynthesis and
289 transcriptional regulation (**Table S7**).

290 Plant hormone signal transduction (Ath04075) involves many hormones that regulate the
291 growth and development, such as auxins, cytokinins, gibberellins, brassinosteroids, jasmonic
292 acid, and ethylene. Twelve DEGs were enriched in the auxin-mediated signalling pathway,
293 including *auxin-responsive protein SAUR* (*SAUR*), *auxin-induced protein X10A* (new gene) and
294 *auxin transporter-like protein* (*LAX*). Among these, *IAA9*, *IAA6*, *SAUR50*, *SAUR32* and
295 *SAUR36* were significantly upregulated. In the cytokinin-mediated signalling pathway, four
296 DEGs were enzyme genes, such as *adenylate isopentenyltransferase 5* (*IPT5*), *7-*
297 *deoxyloganetin glucosyltransferase* (*UGT85A24*), *cytokinin dehydrogenase 6* (*CKX6*), and
298 *cytokinin hydroxylase* (*CYP735A2*). *DELLA protein GAI* (*GAI*), *f-box protein GID2* (*GID2*),
299 and *transcription factor PIF4* (*PIF4*) were enriched in the gibberellin-mediated signalling
300 pathway. *Serine/threonine-protein kinase BSK8* (*BSK8*), *serine/threonine-protein kinase BSK1*
301 (*BSK1*), and *cyclin-D3-3* (*CYCD3-3*) were enriched in the brassinosteroid-mediated signalling
302 pathway. Five DEGs were enriched in the jasmonic mediated signalling pathway, including
303 *Coronatine-insensitive protein homolog 1a* (*COII A*), *protein TIFY6B* (*TIFY6B*), *protein*
304 *TIFY11B* (*TIFY11B*), *protein TIFY10B* (*TIFY10B*), and *protein TIFY3B* (*TIFY3B*). Four

305 upregulated DEGs were enriched in the ethylene-mediated signalling pathway, including
306 *ethylene receptor (ETR1)*, *mitogen-activated protein kinase kinase4 (MKK4)*, *mitogen-*
307 *activated protein kinase homolog MMK1 (MMK1)*, and *protein ethylene insensitive 3 (EIN3)*.

308 Fifteen DEGs were enriched in the photosynthetic pathway (ath00195). Among them,
309 *PPL1*, *PETC*, *PSBR*, *PSBS*, *PSAG*, *PSAO*, *PSB27*, and *PSB28* were related to the photoreaction.
310 *PLSN2* was related to the activity of the chloroplast NAD(P)H dehydrogenase (NDH) complex.
311 *ATPF2* and *ATPC* are related to ATPase activity. Additionally, two oxygen-evolving enhancer
312 proteins and ferredoxins have been identified. In the photosynthesis-antenna protein (ath00196)
313 pathway, eleven DEGs were classified into *chlorophyll a-b binding proteins* and *chlorophyll*
314 *a/b binding proteins*, which were expressed in chloroplasts. In the MAPK signalling (ath04016)
315 pathway, twenty-two DEGs were mainly involved in biotic stress (pathogen infection), abiotic
316 stress (cold/salt/drought/osmotic stress), and hormone synthesis during root growth and
317 wounding responses.

318 Furthermore, the TCA cycle (ath00020), carbon fixation in photosynthetic organisms
319 (ath00710), glycolysis/gluconeogenesis (ath00010), ribosome (ath03010), amino sugar and
320 nucleotide sugar metabolism (ath00520), pyruvate metabolism (ath00620), and
321 phenylpropanoid biosynthesis (ath00940) appeared closely related to alfalfa growth (**Table S7**).
322 In the TCA cycle pathway, 12 DEGs are annotated as playing a role in catalysis of the pyruvate
323 dehydrogenase complex. In addition, *ATP-citrate synthase alpha chain protein 1 (ACLA1)* and
324 *2 malate dehydrogenases (MDH)* were identified. *Pyrophosphate-fructose 6-phosphate 1-*
325 *phosphotransferase subunit beta (PF6P)* and *glycolaldehyde-3-phosphate dehydrogenase*
326 *(GAPC1)*, both members of the glycolysis/gluconeogenesis pathway were highly expressed.
327 Seven *glyceraldehyde-3-phosphate dehydrogenase (GAPDH)* genes were enriched in the
328 “carbon fixation in the photosynthetic organism” pathway and were highly expressed.
329 Ribosomal proteins predominated in the ribosomal pathway and included proteins that are parts
330 of the 30S subunit (*RPS1*, *RPS13*, *RPSQ*, *RPS16*), 40S subunit (*RP24a*, *RP30a*, *RP15d*, *RP10a*,
331 *RP20a*), 50S subunit (*RPL28*, *RPMJ*, *RPL31*, *RPLX*), and 60S subunit (*RPP3a*, *RPL21e*,
332 *RPL37a*, *RPL37B*). *Dihydrolipoyllysine-residue acetyltransferase component 2 of the pyruvate*
333 *dehydrogenase complex* (putative ortholog of *ODP22*) and *malate dehydrogenase (mMDH)*
334 were highly expressed among the pyruvate metabolic pathway genes. *Beta-glucosidase 44*
335 (*BGLU44*), *beta-amylase 1 (BAM1)*, *acid beta-fructofuranosidase (VCINV)*, and *probable*
336 *fructokinase-4 (SCRK4)* were highly expressed among genes in the starch and sucrose
337 metabolism pathways. The genes the phenylpropanoid biosynthesis pathway with high
338 expression were *probable cinnamyl alcohol dehydrogenase (CAD2)*, *beta-glucosidase 46*
339 (*BGLU46*), *trans-cinnamate 4-monooxygenase (CYP73A3)*, and *3 peroxidases (PER)*.

340 **DEGs enriched in a variety of biological processes**

341 All DEGs were analysed using GO and KEGG analyses. We found seven groups of DEGs
342 plausibly related to stem elongation and diameter expansion, including formation of water-
343 conducting tissue in vascular plants, cell division and shoot initiation, biosynthesis and
344 degradation of lignin, cell enlargement and plant growth, formation of the primary or secondary
345 cell wall, cell elongation, and stem growth and induced germination (**Table S8**). Fourteen DEGs
346 were enriched in lignin biosynthesis and degradation. Peroxidases play an important role in this
347 process. Additionally, *peroxidase 47 (PER47)* is a novel gene (**Fig. 6a**). Eleven DEGs were
348 enriched in the formation of the primary or secondary cell wall class. *Cellulose synthase A*

349 *catalytic subunit (CESA)* is up-regulated in WL 712 (**Fig. 6b**). Eighteen DEGs were enriched
350 in the cell enlargement and plant growth category. AUXs, such as *auxin-responsive protein*
351 (*IAA9*), *auxin-induced protein (IAA6)* and *auxin transporter-like protein (LAX5)*, were
352 particularly abundant. Additionally, *auxin-induced protein X10A* is a novel gene (**Fig. 6c**). Five
353 DEGs were enriched in the cell division and shoot initiation category. ~~Enzyme genes such as 7-~~
354 *deoxyloganetin glucosyltransferase (UGT85A24)*, *cytokinin hydroxylase (CYP735A2)* and
355 *cytokinin dehydrogenase 6 (CKX6)* were particularly abundant (**Fig. 7a**). Two DEGs were
356 enriched in the stem growth and induced germination category. Interestingly, one them, *DELLA*
357 *protein (GAI)*, is argued to negatively regulate the gibberellin signalling pathway, whereas the
358 other, *F-Box protein (GID2)*, is supposed to regulate that pathway positively (**Fig. 7b**).
359 *Serine/threonine-protein kinase (BSK1)* and *BSK8* are thought to be related to cell elongation
360 (**Fig. 7c**). *Eukaryotic translation initiation factor 5A-1 (EIF5A)*, *mitogen-activated protein*
361 *kinase kinase kinase 3 (ANP3)*, and *alpha, alpha-trehalose-phosphate synthase (TPS6)* are
362 apparently involved in the formation of water-conducting tissues (**Fig. 7d**). Additionally, we
363 identified genes that are thought to regulate senescence, including *protein ethylene insensitive*
364 *3 (EIN3)* (**Fig. 6d**). Importantly, compared with Aohan, *cellulose synthase A catalytic subunit*
365 *8 (CESA8)*, *beta-1,4-xylosyltransferase (IRX9)*, *probable beta-1,4-xylosyltransferase (IRX14H)*,
366 *auxin-responsive protein (SAUR36)*, *peroxidase 16 (PER16)*, and *peroxidase 51 (PER51)* were
367 upregulated more than 8-fold in WL 712, whereas *mitogen-activated protein kinase 3 (MPK3)*,
368 *pathogenesis-related protein (PR-1)*, *peroxidase 55 (POD55)*, *beta-glucosidase 46 (BGLU46)*,
369 and *peroxidase 15 (POD15)* were downregulated more than 15-fold in WL 712 (**Table S9**). All
370 the genes that might be related to stem growth and development were clustered together, as
371 shown in **Fig. 6** and **Fig. 7**.

372 **Transcription factors potentially involved in alfalfa growth and development**

373 Transcription factors are essential in plant growth and development as protein molecules
374 that regulate gene expression. In this study, 20 transcription factors were implicated in the
375 difference between fast and slow growing alfalfa cultivars (**Fig. 8a, Table S10**). Seven DEGs
376 were upregulated, including *NAC domain-containing protein 73 (NAC073)*, *NAC domain-*
377 *containing protein 10 (NAC010)*, *transcription factor MYB 46 (MYB46)*, and *NAP-related*
378 *protein 2 (NRP2)*. Additionally, *WRKY transcription factor 22 (WRKY22)*, *transcription factor*
379 *TGA 1 (TGA1)* and *transcription factor MYB86* were novel genes. GO annotations state that
380 *NAC073* and *NAC010* are involved in the synthesis of cellulose and hemicellulose and the
381 development of secondary cell wall fibres. Thirteen DEGs were downregulated, and the *WRKY*
382 and *MYB* family members were conspicuous among them. GO classification state that *WRKY51*
383 is involved in the positive regulation of salicylic acid-mediated signal transduction and negative
384 regulation of jasmonic acid-mediated signal transduction in the defense response. *WRKY54* is
385 apparently a negative regulator of plant growth and development. *MYB46* is apparently involved
386 in secondary wall cellulose synthesis as a transcriptional activator. Finally, *MYB86* is apparently
387 involved in lignin synthesis and accumulation. Additionally, *MYB2* is known to inhibit the
388 expression of light-harvesting genes. All identified transcription factors were validated using
389 qRT-PCR (**Fig. 8b**). The relative expression of *NAC081* was significantly upregulated in WL
390 712 plant ($P < 0.001$). The relative expression levels of most transcription factors were similar
391 to the FPKM trend.

392 **The reliability of RNA-seq was verified using qRT-PCR**

393 To determine the accuracy and rationality of the data, we arbitrarily selected 11 DEGs for
394 qRT-PCR validation. The chosen DEGs were mainly related to the formation of the primary or
395 secondary cell wall, cell enlargement and plant growth, and synthesis and degradation of lignin.
396 The changes in transcript abundance are shown in **Fig. 9a**. Consistent with RNAseq, qRT-PCR
397 revealed that *IRX9*, *CESA8*, *CESA7*, *MKK4*, *PER16*, and *PER51* were significantly upregulated
398 in WL 712 plant (P < 0.05). *MPK3*, *PR-1*, *BGLU46*, and *POD15* were significantly
399 downregulated in WL 712 (P < 0.05) (**Fig. 9b**). However, the relative expression of *CAD2*
400 between the two varieties was not significantly different (P > 0.05) and was inconsistent with
401 the RNA-seq transcript abundance. This may have been caused by RNA-seq errors in the
402 acceptable range. Overall, the relative expression trend of the DEGs was similar to the RNA-
403 seq.

404

405 Discussion

406 Alfalfa is an important component of feed, and the growth performance of its aboveground
407 part affects the biomass yield. The *FmS6K* gene plays an important role in regulating the
408 development of plant stems (Sun et al., 2018). The yield of elephant grass has a strong positive
409 correlation with internode length (Yan et al., 2021). However, the molecular regulatory
410 mechanisms underlying the growth rate of stems and branches in alfalfa remain unclear. In this
411 study, the growth difference between the tall and fast growing variety WL 712 and the short
412 and slow-growing variety Aohan was studied. The transcriptome of those two varieties was
413 analyzed by RNA-seq, with RNA obtained from the mid region of the stem. The difference
414 between qRT-PCR and RNA-seq of individual DEGs may be caused by the error of RNA-seq
415 within the acceptable range. Overall, the RNA-seq data could be used for subsequent analysis.
416 All DEGs were associated with at least one GO term; 954 significant DEGs were obtained, and
417 seven DEG clusters were speculated to be involved in promoting fast growth (**Fig. 6, Fig.7**).
418 Additionally, KEGG revealed that hormone signal transduction, photosynthesis and
419 phenylpropanoid biosynthesis genes are up-regulated in the faster growing cultivar. RNA-seq
420 also identified several novel DEGs associated with the fast growing cultivar, including *PER47*
421 and *TIFY10A*.

422 Plant organ growth is influenced by both developmental processes and environmental
423 factors (Sun et al., 2018). In many cases, these changes are due to hormone-mediated action
424 (Verma, Ravindran & Kumar, 2016). Here, auxin, cytokinin, gibberellin, ethylene,
425 brassinosteroid, and jasmonic acid were all implicated because their downstream targets were
426 found among DEGs, such as *SAUR50*, *CKX6*, *GID2*, and *GAI*. These DEGs might play a role
427 in promoting fast growth in alfalfa. Previous studies have identified *SAURs* as a class of
428 hormones that regulate plant growth and development and promote cell enlargement (Ren &
429 Gray, 2015). Cytokinin synthesis is required to activate shoot division in apple trees with the
430 top removed (Tan et al., 2018). Relevant studies have shown that gibberellin regulates plant
431 organ elongation and development (Nagel, 2020). *GAI* is an inhibitor of highly conserved
432 gibberellin signalling in plants. The *SCF (GID2)* complex mediates degradation of DELLA
433 proteins (*RLG2*, *RGA*, and *GAI*), and activates and positively regulates the gibberellin signalling
434 pathway (Dill et al., 2004). In addition, in the plant hormone signal transduction pathway, the
435 production of hormones that play a mediating role depends on the metabolism of amino acids
436 or fatty acids. Tryptophan in plants is not only involved in the synthesis of proteins but also the

437 precursor of many metabolites (such as auxin) (Manol & Nemoto, 2012). Jasmonic acid induces
438 plants to prioritise defense over growth by interfering with the gibberellin signalling cascade,
439 which is usually accompanied by significant growth inhibition (Yang et al., 2012). *TIFY*, which
440 encodes jasmonic acid repressor, was significantly upregulated in Aohan (**Table S7**). This may
441 explain why the Aohan alfalfa is a dwarf plant.

442 Photosynthesis is an essential metabolic process. Twenty-nine DEGs were related to
443 photosynthesis. For example, *PIF1* and *PIF3* were significantly downregulated in WL 712
444 (**Table S7**). These genes may play a regulatory role in the process of plant height and internode
445 elongation. Plant height and leaf area of transgenic soybean are decreased by overexpressing
446 *PIF4* (Arya, Singh & Bhalla, 2021). The deletion of *PIF1* and *PIF3* results in an increase in
447 plant height, longer internodes, and late flowering (Hoang et al., 2021). The light-harvesting
448 complex II (LHC II) functions as a light receptor and is related to the absorption of light (Gu et
449 al., 2017; Sen et al., 2021). The up-regulation of LHC II DEGs may enhance the photosynthesis
450 of WL 712 and promote the growth of plants. Additionally, circadian rhythm is also involved
451 in the regulation of plant growth and development (Venkat & Muneer, 2022). Our research
452 found that DEGs enriched in circadian rhythm pathway were mainly related to photoperiod
453 flowering response. (**Table S7**).

454 RNA-seq analysis found 1531 DEGs related to rape stem growth (Yuan et al., 2019).
455 Combined analysis of proteome and RNA-seq found that DEGs and DEPs of *Mikania*
456 *micrantha* stems were significantly enriched in photosynthesis, carbon sequestration, and plant
457 hormone signal transduction pathways (Can et al., 2021). We identified seven DEG clusters
458 that were plausibly involved in stem elongation and enlargement. Fourteen DEGs were
459 annotated as being involved in lignin synthesis and degradation and peroxidases (**Fig. 6a**).
460 These genes may regulate lignin synthesis and degradation in stems. The oxidation activity of
461 peroxidases is important for lignification (Hoffmann et al., 2020). Eleven DEGs were
462 apparently involved in the formation of the primary or secondary cell wall (**Fig. 6b**), with good
463 representation from cellulose synthase. Previous studies reported that *CESA 4* and *CESA8* are
464 specifically enriched and expressed in the stem tissue during the fiber development stage (Guo
465 et al., 2021). Eighteen DEGs were enriched in the category of cell enlargement and plant growth
466 frequently involving auxin (**Fig. 6c**). Five DEGs were apparently involved in cell division and
467 shoot initiation (**Fig. 7a**). Two DEGs were enriched in the categories of stem growth and
468 induced germination (**Fig. 7b**), mainly components of the gibberellin signalling pathway. Two
469 DEGs were potentially involved in cell elongation (**Fig. 7c**). These DEGs might play a role in
470 stem internode elongation, diameter enlargement and lateral branch formation. Previous studies
471 reported that *AtTPS6* completely compensates for the defects in reduced trichome and stem
472 branching due to *CSP-1* deficiency in *Arabidopsis thaliana* (Chary et al., 2008). Deletion of
473 *IAA17* in tomatoes showed that the increase in fruit size is related to the higher ploidy level of
474 peel cells (Su et al., 2015). Finally, the *TIFY* homologs possibly involved in senescence were
475 also identified here (**Fig. 6d**). In addition, we identified several members of *SPL* family, such
476 as *SPL1*, *SPL6* and *SPL7*, which may be involved in the lateral branch development of alfalfa.
477 Previous studies reported that *SPL13* regulates shoot branching in alfalfa (Gao et al., 2018).
478 Overall, these DEGs may be involved in alfalfa growth and development.

479 Transcription factors are essential in the regulation of development, morphogenesis and
480 responses to environmental stress. Previous research found that most members of *NAC*, *WRKY*

481 and *MYB* families are involved in the synthesis of lignin, cellulose, and hemicellulose (Wang
482 et al., 2016). The *NAC*-mediated transcription network synergistically regulates synthesis of the
483 plant secondary wall (Ryan, Zhong & Ye, 2011). *WRKY6* and *WRKY33* positively regulated
484 abscisic acid signal transduction during early development of *A. thaliana* (Huang et al., 2016).
485 *WRKY54* is a negative regulator of salicylic acid synthesis (Li, Zhong & Palva, 2017) and can
486 significantly increase stem diameter, leaf area, and total dry weight of plants (Amin et al., 2013).
487 Overexpression of *AtMYB44* in tomatoes results in slow growth (Shim et al., 2012). *MYB3R1*
488 is a transcriptional repressor that regulates organ growth, and restricts plant growth and
489 development by binding to target genes and promoters of specific genes (Wang et al., 2018).
490 Under reduced light intensity, *MYB2* and *MYR1* act as inhibitors of flowering and organ
491 elongation, respectively (Zhao et al., 2011). Here, excluding *WRKY22*, all *WRKY* members
492 were significantly upregulated in dwarf alfalfa. Therefore, *WRKY22* may positively regulate the
493 growth and development of WL 712. *NACs* are involved in the development of plant secondary
494 cell walls. Among these, *NAC081* functions as a positive regulator. *MYB46* and *MYB86* might
495 positively regulate the synthesis of cellulose and lignin, and *MYB44*, *MYB3R1* and *MYB2* might
496 act as transcriptional repressors (**Table S10**).

497

498 **Conclusion**

499 Plant height is an important factor in determining forage biomass. The molecular
500 characteristics of the DEGs between fast and slow growing alfalfa cultivars were identified
501 using RNA-seq. The trend of our qRT-PCR was largely consistent with those of RNA-seq,
502 which indicated that the RNA-seq data could be used for subsequent analysis. All DEGs were
503 analysed using GO terms, and 954 significant DEGs were identified. KEGG analysis indicated
504 that hormone signal transduction, phenylpropanoid biosynthesis, and photosynthesis are well
505 represented in the fast growing cultivar. GO analysis highlighted the following seven clusters
506 of DEGs: formation of water-conducting tissue, cell division and shoot initiation, synthesis and
507 degradation of lignin, stem growth, formation of the primary or secondary cell wall, cell
508 enlargement and plant growth, and induced germination and cell elongation. Additionally, the
509 transcription factors implicated in stem elongation and diameter expansion are mainly *WRKY*,
510 *NAC*, and *MYB* family members. In summary, our research results not only enrich the
511 transcriptome database of alfalfa, but also provide valuable information for explaining the
512 molecular mechanism of fast growth, and can provide reference for the production of alfalfa
513 around the world.

514 **Competing Interests**

515 The authors declare there are no competing interests.

516 **Author Contributions**

517 Qi Jiangjiao conceived and designed the experiments, performed the experiments,
518 analyzed the data, prepared figures or tables, and authored or reviewed drafts of the paper.

519 Yuxue, Wang Xuzhe and Zhang Fanfan performed the experiments.

520 Ma Chunhui conceived and designed the experiments, performed the experiments,
521 analyzed the data, authored or reviewed drafts of the paper, and approved the final draft.

522 **Availability of data and materials**

523 The data is available at the Sequence Read Archive (SRA) of NCBI:

524 <https://www.ncbi.nlm.nih.gov/sra/?term=PRJNA807394>.

525 **Funding**

526 This work was supported by China Agriculture Research System of MOF and MARA.

527

528 **References**

- 529 Aung B, Gruber M, Amyot L, Omari K, Bertrand A, Hannoufa A. 2015. Ectopic expression of
530 LjmiR156 delays flowering, enhances shoot branching, and improves forage quality in
531 alfalfa. *Plant Biotechnology Reports* 9(6):379-393
- 532 Arshad M, Gruber MY, Hannoufa A. 2018. Transcriptome analysis of microRNA156
533 overexpression alfalfa roots under drought stress. *Scientific Reports* 8:9363-9375
- 534 Arya H, Singh MB, Bhalla PL. 2021. Overexpression of PIF4 affects plant morphology and
535 accelerates reproductive phase transitions in soybean. *Food and Energy Security* 10(3):1-
536 15
- 537 Amin AA, El-Kader AA Abd, Shalaby MAF, Gharib FAE, Rashad ESM, Teixeira da SJA. 2013.
538 Physiological effects of salicylic acid and thiourea on growth and productivity of maize
539 plant in sandy soil. *Communications in Soil Science & Plant Analysis* 44(7):1141-1155
- 540 Bambang S, Lukmana A, Nafiatul U, Bambang S. 2021. The performance and genetic variation
541 of first and second generation tropical alfalfa (*Medicago sativa*). *Biodiversitas* 22(6):3265-
542 3270
- 543 Celebi SZ, Kaya L, Sahar AK, Yergin R. 2010. Effects of the weed density on grass yeild of
544 alfalfa in different row spacing applications. *African Journal of Biotechnology* 9(41):6867-
545 6872
- 546 Chen L, Yang Y, K Mishina, Cui C, Zhao Z, Duan S, Chai Y, Su R, Chen F, Hu Y.G. 2020.
547 RNA-seq analysis of the peduncle development of Rht12 dwarf plants and primary mapping
548 of Rht12 in common wheat. *Cereal Research Communications* 48(2):139-147
- 549 Cui C, Wang Z, Su YJ, Wang T. 2021. New insight into the rapid growth of the *Mikania*
550 *micrantha* stem based on DIA proteomic and RNA-seq analysis. *Journal of Proteomics*
551 236:104126-104140
- 552 Chary SN, Hicks GR, Choi YG, Carter D, Raikhel NV. 2008. Trehalose-6-phosphate
553 synthase/phosphatase regulates cell shape and plant architecture in Arabidopsis. *Plant*
554 *Physiology* 146(1):97-107
- 555 Diatta AA, Doohong M, Jagadish SVK. 2021. Drought stress responses in non-transgenic and
556 transgenic alfalfa--current status and future research directions. *Advances in Agronomy*
557 170:35-100
- 558 Dill A, Thomas SG, Hu JH, Steber CM, Sun TP. 2004. The Arabidopsis F-box protein
559 SLEEPY1 targets gibberellin signaling repressors for gibberellin-induced degradation.
560 *Plant Cell* 16(6):1392-1405
- 561 Ernest BA, Alena PB, Mariam RS, Marian O, Edo G, Henk VA, Richard GFV, C Gerard VDL.
562 2020. Morphological and physiological responses of the potato stem transport tissues to
563 dehydration stress. *Planta* 251(2):45-59
- 564 Etzold S, Sterck F, Bose AK, Braun S, Buchmann N, Eugster W, Gessler A, Kahmen A, Peters
565 RL, Vitasse Y, Walthert L, Ziemińska Kasia, Zweifel R, Penuelas J. 2021. Number of
566 growth days and not length of the growth period determines radial stem growth of temperate
567 trees. *Ecology Letters* 25:427-439
- 568 Fan WQ, Ge GT, Liu YH, Wang W, Liu LY, Jia YS. 2018. Proteomics integrated with

- 569 metabolomics: analysis of the internal causes of nutrient changes in alfalfa at different
570 growth stages. *BMC Plant Biology* 18 (1):78-92
- 571 Gao RM, Austin RS, Amyot L, Hannoufa A. 2016. Comparative transcriptome investigation of
572 global gene expression changes caused by miR156 overexpression in *Medicago sativa*.
573 *BMC Genomics* 17(1):658-672
- 574 Guo JD, Huang Z, Sun JL, Cui XM, Liu Y. 2021. Research progress and future development
575 trends in medicinal plant transcriptomics. *Frontiers in Plant Science* 12:691838-691847
- 576 Gu JF, Zhou ZX, Li ZK, Chen Y, Wang ZQ, Zhang H, Yang JC. 2017. Photosynthetic properties
577 and potentials for improvement of photosynthesis in pale green leaf rice under high light
578 conditions. *Frontiers in Plant Science* 8:1082-1095
- 579 Hoang QTN, Tripathi S, Cho JY, Choi DM, Shin AY, Kwon SY, Han YJ, Kim JI. 2021.
580 Suppression of phytochrome interacting factors enhance photoresponses of seedlings and
581 delays flowering with increased plant height in brachypodium distachyon. *Frontiers in*
582 *Plant Science* 12:756795-756811
- 583 Hoffmann N, Benske A, Betz H, Schuetz M, Samuels AL. 2020. Laccases and peroxidases co-
584 localize in lignified secondary cell walls throughout stem development. *Plant Physiology*
585 184(2):806-822
- 586 Huang Y, Feng CZ, Ye Q, Wu WH, Chen YF. 2016. Arabidopsis WRKY6 transcription factor
587 acts as a positive regulator of abscisic acid signaling during seed germination and early
588 seedling development. *PLoS Genetics* 12(2):1-22
- 589 Jaykumar JC, Mahendra LA. 2016. In vitro callus induction and plant regeneration from stem
590 explants of *Ceropegia noorjahaniae*, a critically endangered medicinal herb. *Methods in*
591 *Molecular Biology* 1391:347-355
- 592 Kleyer M, Trinogga J, Cebrin-Piqueras MA, Trenkamp A, Fljgaard C, Ejrns R, Bouma TJ,
593 Minden V, Maier M, Mantilla CJ, Albach DC, Blasius B, Barua D. 2019. Trait correlation
594 network analysis identifies biomass allocation traits and stem specific length as hub traits
595 in herbaceous perennial plants. *Journal of Ecology* 107(2):829-842
- 596 Kumar T, Bao AK, Bao Z, Wang F, Gao L, Wang SM. 2018. The progress of genetic
597 improvement in alfalfa (*Medicago sativa* L). *Czech Journal of Genetics and Plant Breeding*
598 54(2):41-51
- 599 Kim S, Cho K, Lim SH, Goo TW, Lee JY. 2021. Transcriptome profiling of transgenic rice
600 seeds lacking seed storage proteins (globulin, prolamin, and glutelin) by RNA-seq analysis.
601 *Plant Biotechnology Reports* 15(1):77-93
- 602 Katyayini NU, Rinne PLH, Tarkowska D, Strnad M, Schoot C. 2020. Dual role of gibberellin
603 in perennial shoot branching: inhibition and activation. *Frontiers in Plant Science* 11:736-
604 753
- 605 Livak KJ, Schmittgen TD. 2001. Analysis of relative gene expression data using real-time
606 quantitative PCR and the $2^{-\Delta\Delta CT}$ method. *Methods* 25(4):402-408
- 607 Li J, Zhong R, Palva ET. 2017. WRKY70 and its homolog WRKY54 negatively modulate the
608 cell wall-associated defenses to necrotrophic pathogens in Arabidopsis. *PLoS One* 12(8):1-
609 22
- 610 Martin N, Brink G, Shewmaker G, Undersander D, Walgenbach R, Hall M. 2010. Changes in
611 alfalfa yeild and nutritive value within individual harvest periods. *Agronomy Journal*
612 102(4):1274-1282

- 613 Monirifar H. 2011. Path analysis of yeild and quality traits in alfalfa. *Notulae Botanicae Horti*
614 *Agrobotanici Cluj-Napoca* 39(2):190-195
- 615 Mortazavi A, Williams BA, McCue K. 2008. Mapping and quantifying mammalian
616 transcriptomes by RNA-seq. *Nature Methods* 5(7):621-628
- 617 Mano Y, Nemoto K. 2012. The pathway of auxin biosynthesis in plants. *Journal of*
618 *Experimental Botany* 63:2853-2872
- 619 Nagel R. 2020. Gibberellin signaling in plants:entry of a new microRNA player. *Plant*
620 *Physiology* 183(1):5-6
- 621 Pablo PG, Miguel AMR. 2018. Stem cells and plant regeneration. *Developmental Biology*
622 442(1):3-12
- 623 Ren H, Gray WM. 2015. SAUR proteins as effectors of hormonal and environmental signals in
624 plant growth. *Molecular Plant* 8(8):1153-1164
- 625 Ryan LM, Zhong RQ, Ye ZH. 2011. Secondary wall NAC binding element (SNBE), a key cis-
626 acting element required for target gene activation by secondary wall NAC master switches.
627 *Plant Signaling & Behavior* 6(9):1282-1285
- 628 Sulc RM, Arnold AM, Cassida KA, Albrecht KA, Hall MH, Min D, Xu X, Undersander DJ,
629 Santen E. 2021. Changes in forage nutritive value of reduced-lignin alfalfa during regrowth.
630 *Crop Science* 61(2):1478-1487
- 631 Sun H, Zhao XT, Liu Z, Yang K, Wang Y, Zhan YG. 2018. Bioinformatics of S6K genes in
632 *Fraxinus mandshurica* and their expression analysis under stress and hormone. *Plant*
633 *Research* 38(5):714-724
- 634 Sen S, Mascoli V, Liguori N, Croce R, Visscher L. 2021. Understanding the relation between
635 structural and spectral properties of light harvesting complex II. *The Journal of Physical*
636 *Chemistry. A* 125(0):4313-4322
- 637 Su LY, Audran C, Bouzayen M, Roustan JP, Chervin C. 2015. The Aux/IAA, SI-IAA17
638 regulates quality parameters over tomato fruit development. *Plant Signaling & Behavior*
639 10(11):e1071001-e1071009
- 640 Shim JS, Jung C, Lee S, Min K, Lee YW, Choi Y, Lee JS, Song JT, Kim JK, Choi YD. 2012.
641 AtMYB44 regulates WRKY70 expression and modulates antagonistic interaction between
642 salicylic acid and jasmonic acid signaling. *The Plant Journal* 73(3):483-495
- 643 Trapnell C, Roberts A, Goff L, Pertea G, Kim D, Kelley DR, Pimentel H, Salzberg SL, Rinn
644 JL, Pachter L. 2012. Differential gene and transcript expression analysis of RNA-seq
645 experiments with TopHat and Cufflinks. *Nature Protocols* 7:562-578
- 646 Tetteh JP, Bonsu KO. 1997. Agronomic performance of seven cultivars of alfalfa (*Medicago*
647 *sativa L.*) in the coastal savanna zone of Ghana. *Ghana Journal of Agricultural Science*
648 30(1):39-44
- 649 Tan M, Li GF, Qi SY, Liu XJ, Chen XL, Ma JJ, Zhang D, Han MY. 2018. Identification and
650 expression analysis of the IPT and CKX gene families during axillary bud outgrowth in
651 apple (*Malus domestica* Borkh). *Gene* 651:106-117
- 652 Verma V, Ravindran P, Kumar PP. 2016. Plant hormone-mediated regulation of stress
653 responses. *BMC Plant Biology* 16(1):1-10
- 654 Venkat A, Muneer S. 2022. Role of circadian rhythms in major plant metabolic and signaling
655 pathways. *Frontiers in Plant Science* 13:836244-836254
- 656 Wang J, Tang F, Gao CP, Gao X, Xu B, Shi FL. 2021. Comparative transcriptome between male

- 657 fertile and male sterile alfalfa (*Medicago varia*). *Physiology and Molecular Biology of*
658 *Plants* 27(7):1487-1498
- 659 Wang YJ, Li MC, Wu Wang, Wu HY, Xu YN. 2013. Cloning and characterization of an
660 AP2/EREBP gene TemAP2-1 from *Tetraena mongolica*. *Bulletin of Botany* 48(1):23-33
- 661 Wang HZ, Yang JH, Chen F, Torres-Jerez I, Tang YH, Wang MY, Du Q, Cheng XF, Wen JQ,
662 Dixon R. 2016. Transcriptome analysis of secondary cell wall development in *Medicago*
663 *truncatula*. *BMC Genomics* 17:23-37
- 664 Wang WP, Sijacic P, Xu PB, Lian HL, Liu ZC. 2018. Arabidopsis TSO1 and MYB3R1 form a
665 regulatory module to coordinate cell proliferation with differentiation in shoot and root.
666 *Proceedings of the National Academy of Sciences of the United States of America*
667 115(13):e3045-e3054
- 668 Yu L, Chen HW, Hong PP, Wang HL, Liu KF. 2015. Adventitious bud induction and plant
669 regeneration from stem nodes of *Salvia splendens* 'Cailinghong'. *Hortscience* 50:869-872
- 670 Yuan JB, Sun XB, Guo T, Chao YH, Han LB. 2020. Global transcriptome analysis of alfalfa
671 reveals six key biological processes of senescent leaves. *Peer Journal* 8(1):e8426-e8448
- 672 Yu KMJ, McKinley B, Rooney WL, Mullet JE. 2021. High planting density induces the
673 expression of GA3-oxidase in leaves and GA mediated stem elongation in bioenergy
674 sorghum. *Scientific Reports* 11(1):46-58
- 675 Yan Q, Li J, Lu LY, Gao LJ, Lai DW, Yao N, Yi XF, Wu ZY, Lai ZQ, Zhang JY. 2021. Integrated
676 analyses of phenotype, phytohormone, and transcriptome to elucidate the mechanism
677 governing internode elongation in two contrasting elephant grass (*Cenchrus purpureus*)
678 cultivars. *Industrial Crops & Products* 170:113693-113702
- 679 Yuan R, Zeng XH, Zhao SB, Wu G, Yan XH. 2019. Identification of candidate genes related to
680 stem development in *Brassica napus* using RNA-seq. *Plant Molecular Biology Reporter*
681 37(4):347-364
- 682 Ziliotto U, Leinauer B, Lauriault LM, Rimi F, Macolino S. 2010. Alfalfa yeild and morphology
683 of three fall dormancy categories harvested at two phenological stages in a subtropical
684 climate. *Agronomy Journal* 102(6):1578-1585
- 685 Zhang H, Liu XQ, Wang XM, Sun M, Song R, Mao PS, Jia SG. 2021. Genome-wide
686 identification of GRAS genes family and their responses to abiotic stress in *Medicago sativa*.
687 *International Journal of Molecular Sciences* 22(14):7729-7749
- 688 Zheng XM, Chen YJ, Zhou YF, Shi KK, Hu X, Li DY, Ye HZ, Zhou Y, Wang K. 2021. Full-
689 length annotation with multistrategy RNA-seq uncovers transcriptional regulation of
690 lncRNAs in cotton. *Plant Physiology* 185(1):179-195
- 691 Zhao CS, Atsushi H, Shinjiro Y, Kamiya Yuji, Beers EP. 2011. The Arabidopsis MYB genes
692 MYR1 and MYR2 are redundant negative regulators of flowering time under decreased
693 light intensity. *Plant Journal* 66(3):502-515

Figure 1

Slow-growing Aohan and vigorous-growing WL 712 plants at bud stage.

Soil grown plants, approximately 60 days after planting.

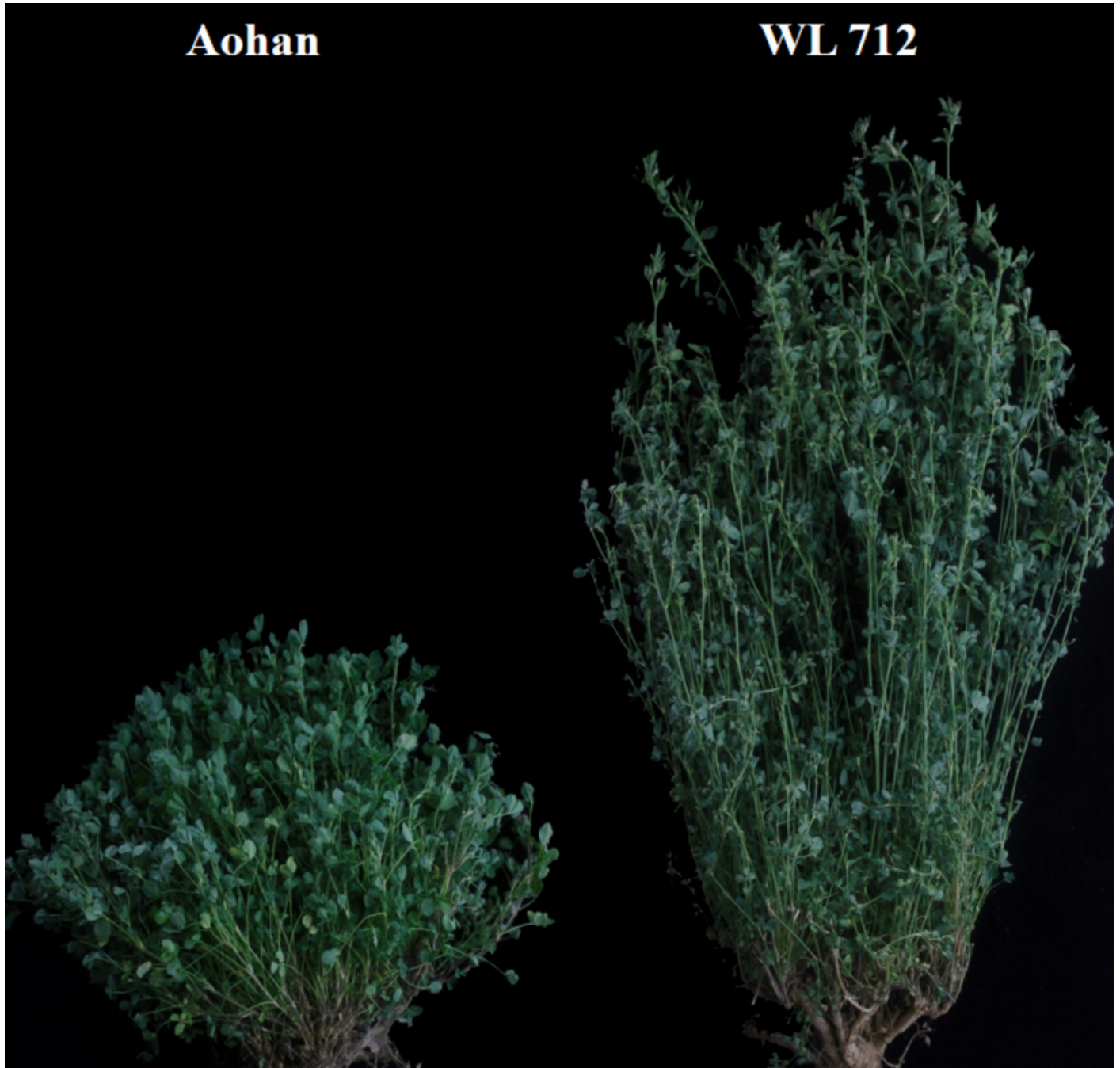


Figure 2

Phenotypic evaluation of five alfalfa cultivars.

The dynamics of plant height (a), stem diameter (b) and internode length (c) of five alfalfa cultivars during the indicated stages of development. Here, we recorded the transplanting stage as 0 day, branching stage (18 d), budding stage (42 d), early flower stage (45 d) and full flower stage (50 d). Average plant height (d), stem diameter (e), internode length (f) of five alfalfa cultivars. The values are the average of fifteen biological replicates and error bars represent the standard deviation. Different letters indicate significant difference at $P < 0.05$ among the five cultivars as determined by Student's t test.

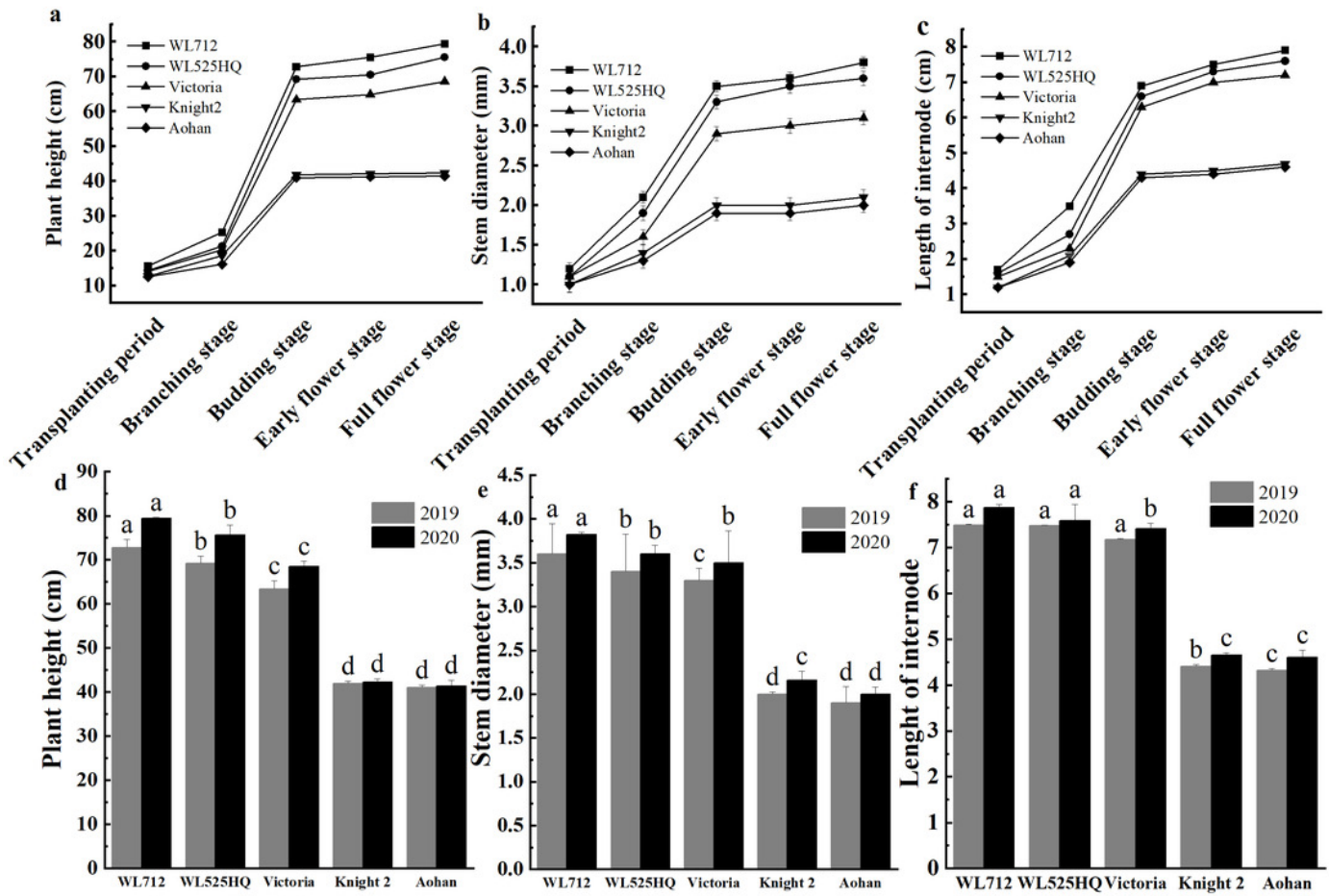


Figure 3

Phenotypic evaluation and index determination of five alfalfa cultivars at budding stage (42 d).

Lateral branch number (a), total branch number (b), leaf area (c), fresh weight (d), leaf to stem ratio (e) and dry weight (f) of five alfalfa cultivars. The values are the average of fifteen biological replicates and error bars represent the standard deviation. Different letters indicate significant difference at $P < 0.05$ among the five cultivars as determined by Student's t test.

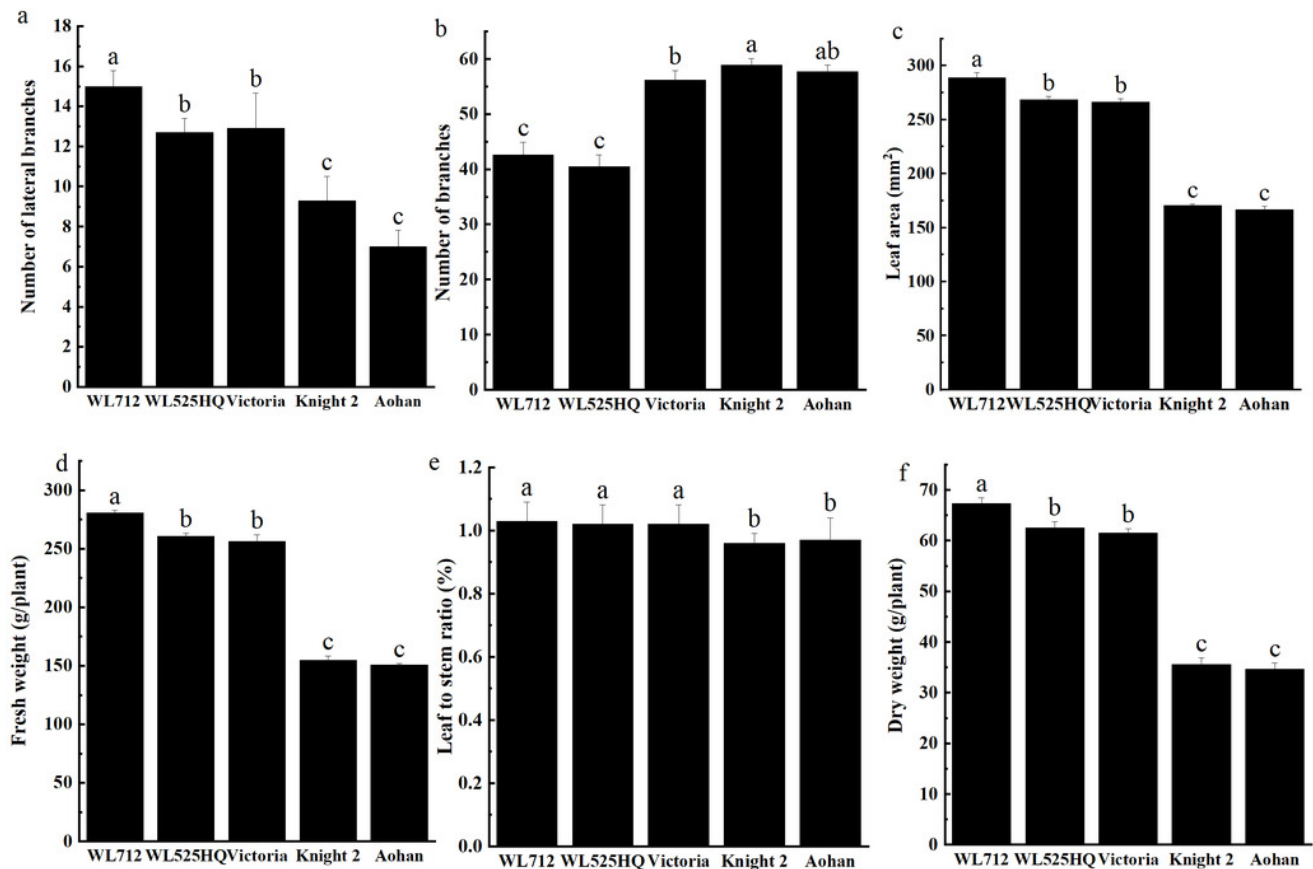


Figure 4

Scatter diagram of enriched GO functional categories.

The “GeneRatio” shows the ratio of the number of DEGs in the given category to the total number of differentially expressed genes. The size of the spot indicates the approximate number of DEGs in the category, all the spots indicate the significance level, $P < 0.05$.

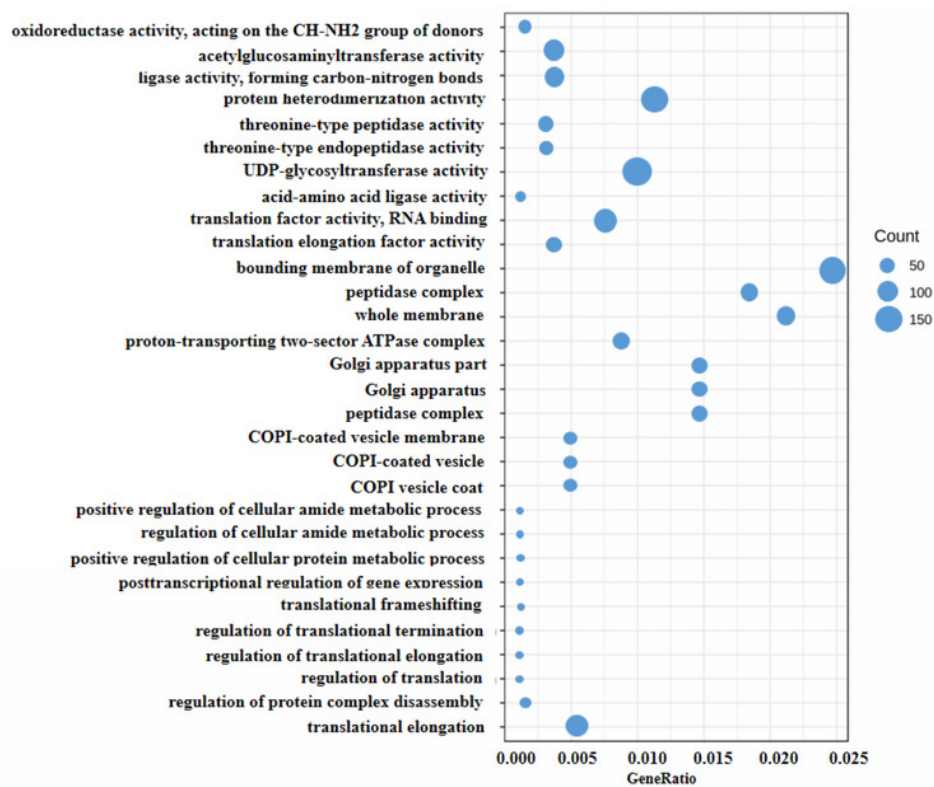


Figure 5

KEGG classification of differentially expressed genes (DEGs).

X-axis is the number of gene annotations; Y-axis is the type of KEGG pathway.

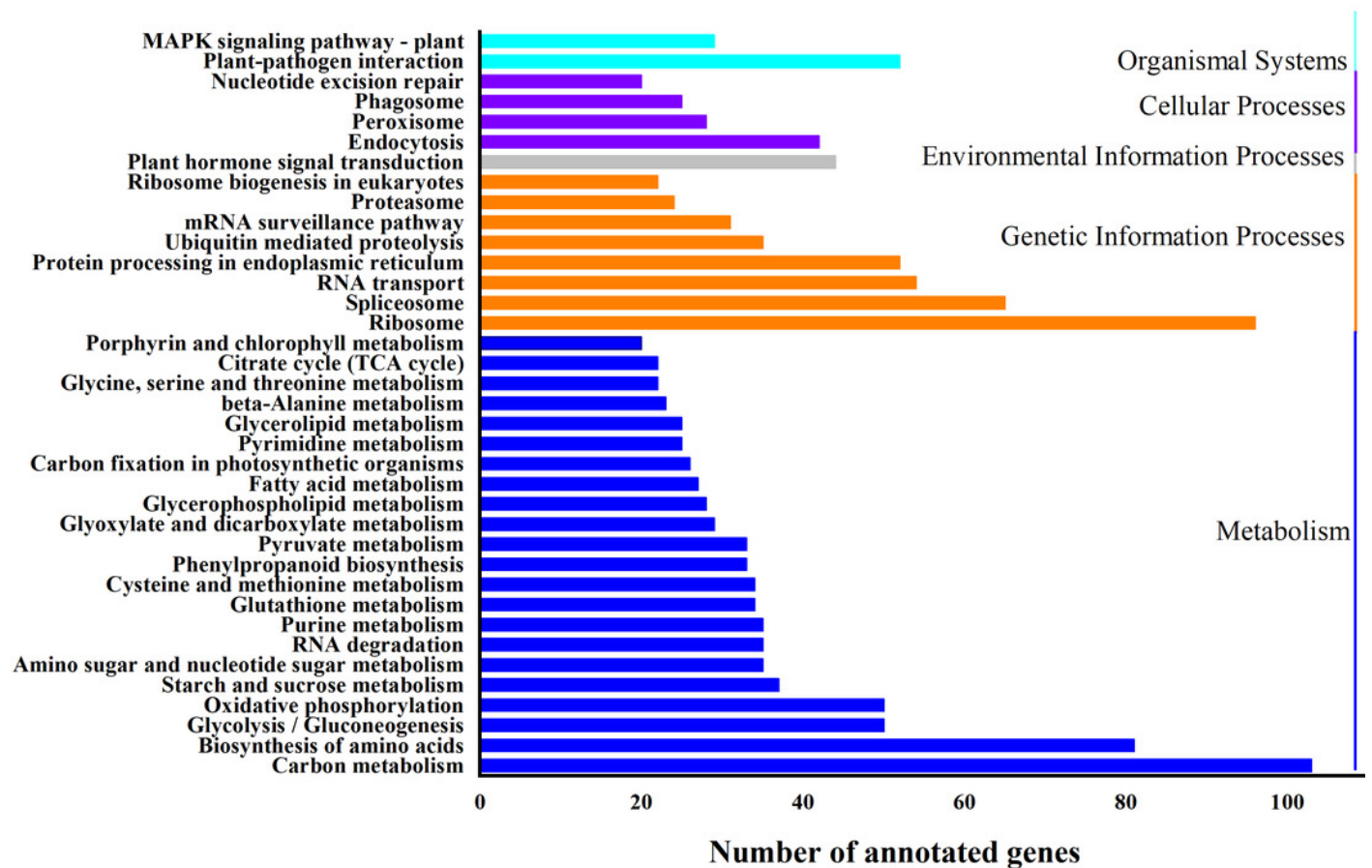


Figure 6

Bar graphs showing the FPKM (fragments per kilobase of transcript per million mapped reads) of DEGs involved in various biological processes distinguished by GO enrichment analysis.

(a) Synthesis and degradation of lignin; (b) Formation of the primary cell wall or secondary cell wall; (c) Cell enlargement and plant growth; (d) Senescence.

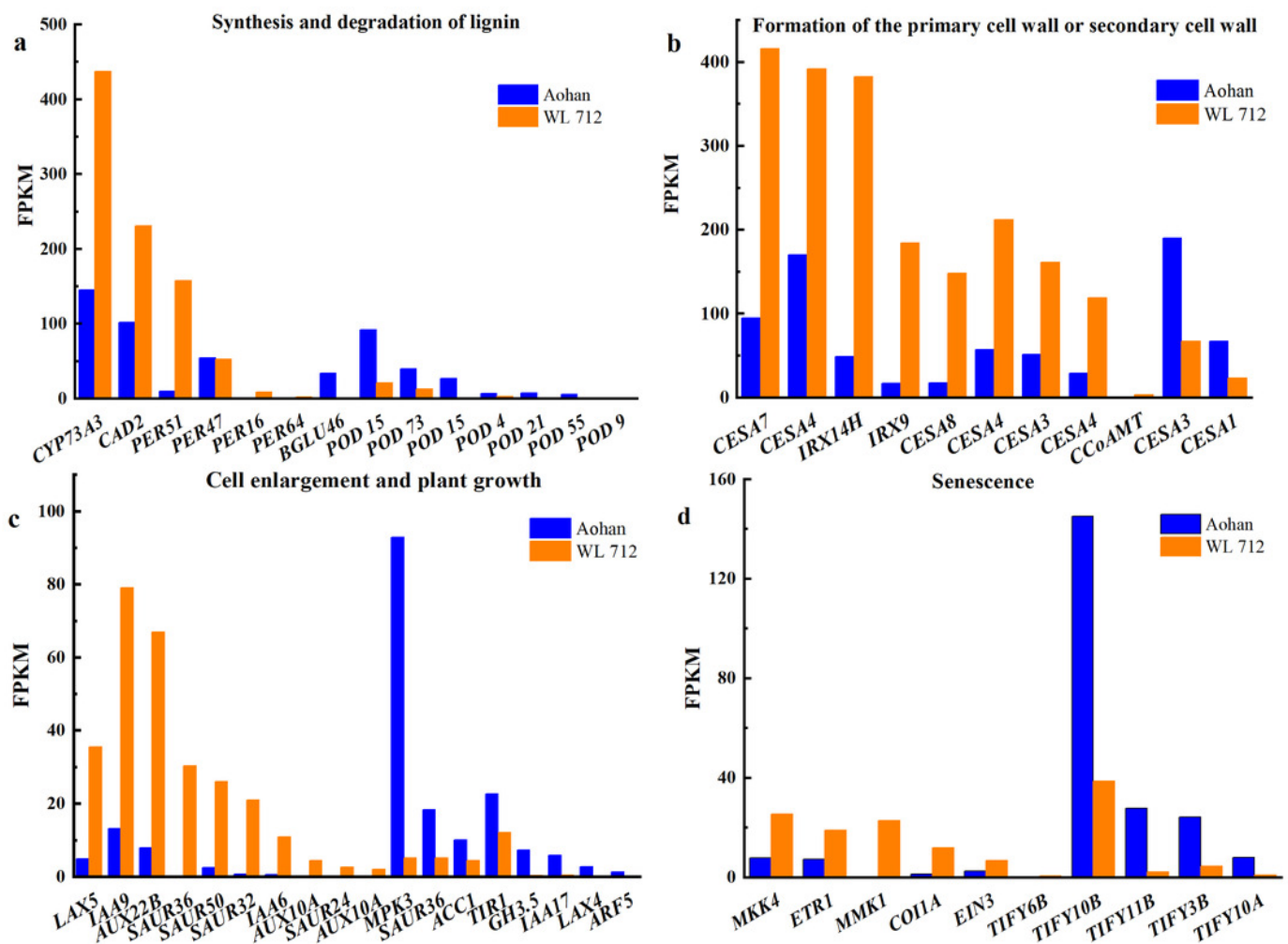


Figure 7

Bar graphs showing the FPKM of DEGs involved in additional biological processes distinguished by GO enrichment analysis.

(a) Cell division and shoot initiation; (b) Stem growth and induced germination; (c) Cell elongation; (d) Formation of water-conducting tissues.

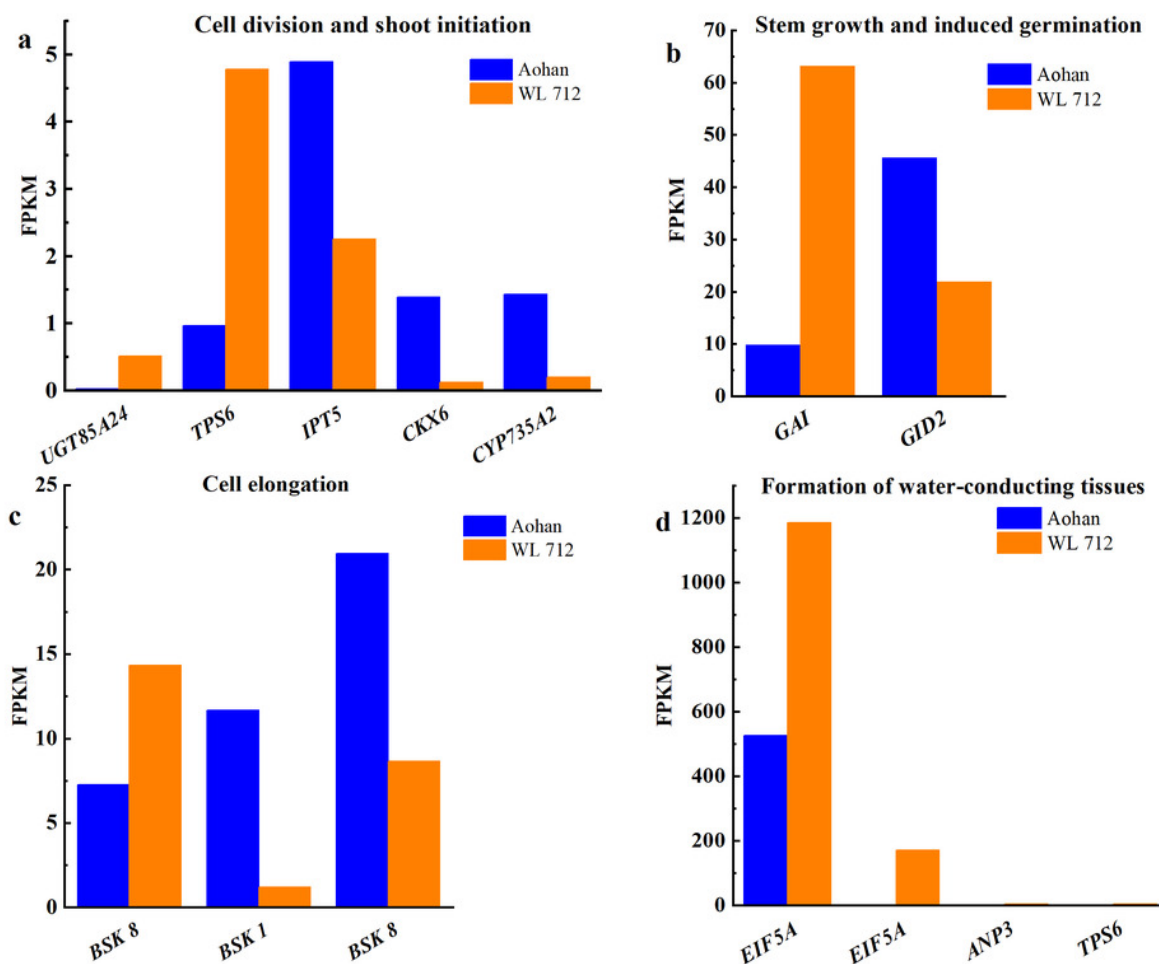


Figure 8

Transcription factors putatively involved in stem elongation and diameter enlargement in alfalfa as distinguished by GO analysis.

(a) Bar graphs showing the transcript abundance based on FPKM. (b) Bars plot the relative expression levels based on qPCR. *, **, *** Expression level of the cultivars is significantly different at the 0.05, 0.01, and 0.001 probability levels, respectively. The expression levels of all genes are plotted relative to the expression level of the internal standard (β -Actin).

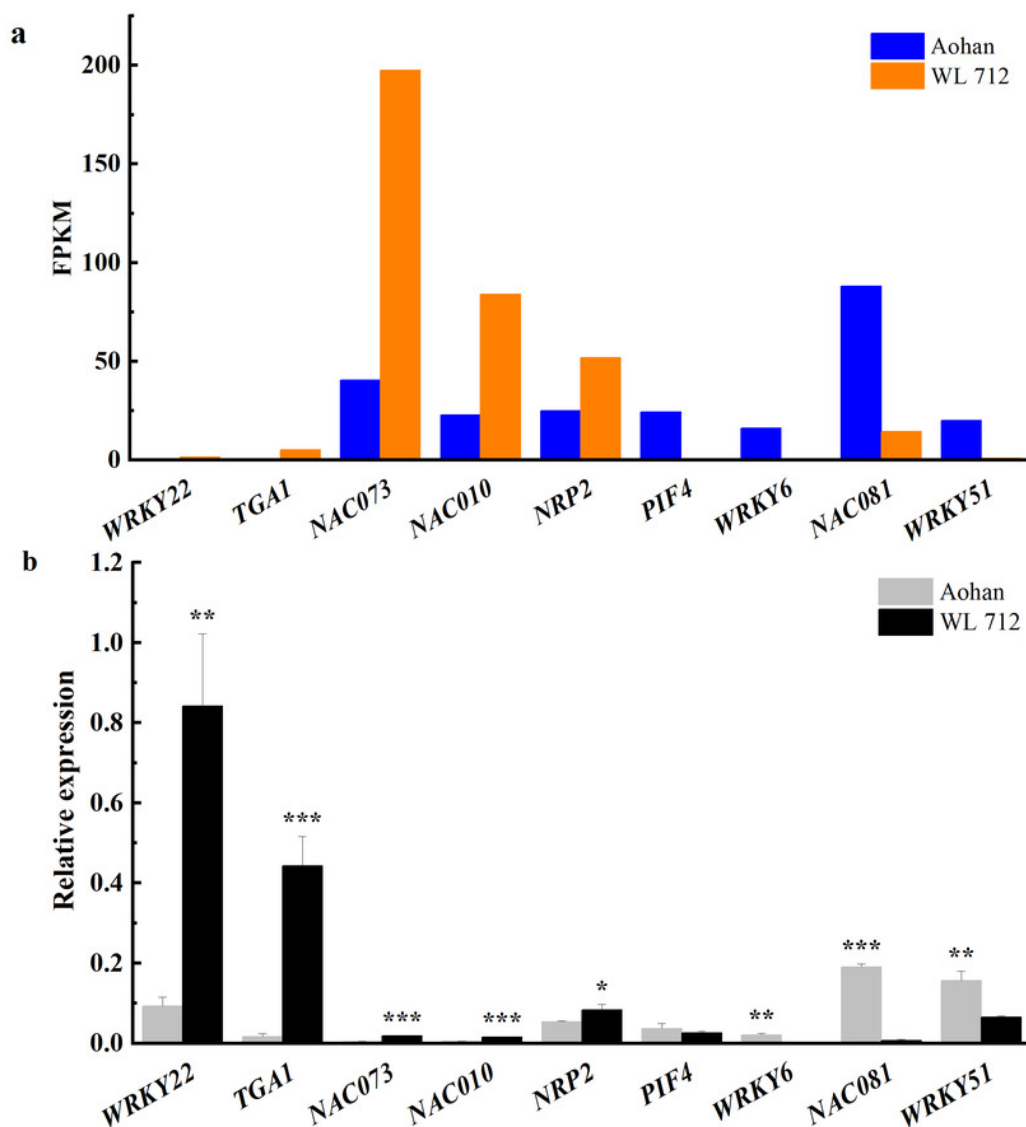


Figure 9

Comparison of RNA-seq and qRT-PCR for 11 genes.

(a) RNAseq bars show transcript abundance based on FPKM. (b) qRT-PCR bars show transcript abundance based on qRT-PCR. *, *** Expression level of the cultivars is significantly different at the 0.05, and 0.001 probability levels, respectively. The expression levels of all genes are plotted relative to the expression level of the internal standard (β -Actin).

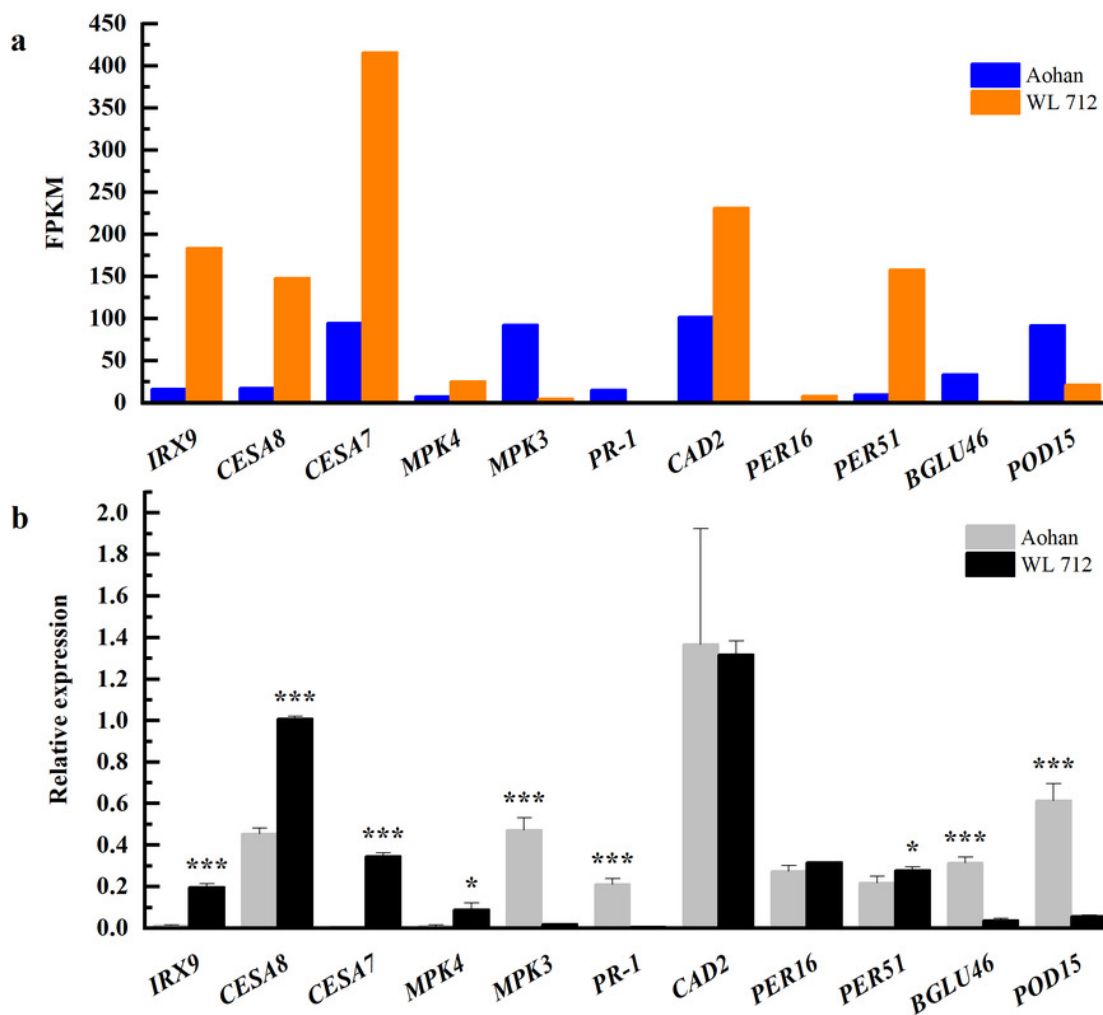


Table 1 (on next page)

The growth index of the two varieties in greenhouse-grown plants

Different letters indicate significant difference at $P < 0.05$ among the two varieties as determined by Student's t test.

1 Table 1 The growth index of the two varieties in greenhouse-grown plants
2

	Plant Height (cm)	Length of Internodde (cm)	Stem Diameter (mm)	Leaf Areas (mm²)	Plant Weight (g/plant)
WL 712	50.2 ± 1 ^a	5.14 ± 0.09 ^a	2.52 ± 0.022 ^a	159 ± 0.6 ^a	231 ± 2.4 ^a
Aohan	28.7 ± 1 ^c	2.94 ± 0.07 ^c	1.19 ± 0.027 ^c	127 ± 2.8 ^c	141 ± 0.4 ^c

3

4 Different letters indicate significant difference at $P < 0.05$ among the two varieties as determined by Student's t test.

Table 2 (on next page)

Correlation coefficients between traits among the five alfalfa cultivars

*, ** Significant at the 0.05, and 0.01 probability levels, respectively. PH, plant height; IL, internode length; SD, stem diameter; FW, fresh weight; LSR, leaf-to-stem ratio; DW, dry weight; LBN, lateral branch number; MBN, main branch number.

Table 2. Correlation coefficients between traits among the five alfalfa cultivars

	PH	SD	IL	LBN	MBN	FW	LSR	DW
PH	1							
SD	0.98**	1						
IL	0.99**	0.98**	1					
LBN	0.89**	0.92**	0.90**	1				
MBN	-0.84**	-0.76**	-0.79**	-0.68**	1			
FW	0.98**	0.98**	0.98**	0.91**	-0.75**	1		
LSR	0.55**	0.54**	0.55**	0.51**	-0.46*	0.60**	1	
DW	0.99**	0.99**	0.99**	0.82**	-0.76**	1.00**	0.59**	1

*, ** Significant at the 0.05, and 0.01 probability levels, respectively.

PH, plant height; IL, internode length; SD, stem diameter; FW, fresh weight; LSR, leaf-to-stem ratio; DW, dry weight; LBN, lateral branch number; MBN, main branch number.

Table 3 (on next page)

Top 10 gene ontology function classification

Table 3 Top 10 gene ontology function classification

Category	Description	GO ID	Count	Percentage(%)
Biological process	translational elongation	GO:0006414	41	4.30
	regulation of protein complex disassembly	GO:0043244	8	0.84
	regulation of translation	GO:0006417	7	0.73
	regulation of translational elongation	GO:0006448	7	0.73
	regulation of translational termination	GO:0006449	7	0.73
	translational frameshifting	GO:0006452	7	0.73
	posttranscriptional regulation of gene expression	GO:0010608	7	0.73
	positive regulation of cellular protein metabolic process	GO:0032270	7	0.73
	regulation of cellular amide metabolic process	GO:0034248	7	0.73
	positive regulation of cellular amide metabolic process	GO:0034250	7	0.73
Cell component	bounding membrane of organelle	GO:0098588	57	5.97
	peptidase complex	GO:1905368	44	4.61
	whole membrane	GO:0098805	49	5.13
	proton-transporting two-sector ATPase complex	GO:0033177	20	2.10
	Golgi apparatus part	GO:0044431	36	3.77
	Golgi apparatus	GO:0005794	36	3.77
	proteasome core complex	GO:0005839	37	3.88
	COPI-coated vesicle membrane	GO:0030126	9	0.94
	COPI-coated vesicle	GO:0030137	9	0.94
COPI vesicle coat	GO:0030126	9	0.94	
Molecular function	translation elongation factor activity	GO:0003746	41	4.30
	translation factor activity, RNA binding	GO:0008135	86	9.01
	acid-amino acid ligase activity	GO:0016881	12	1.26
	UDP-glycosyltransferase activity	GO:0008194	99	1.04
	threonine-type endopeptidase activity	GO:0004298	37	3.88
	threonine-type peptidase activity	GO:0070003	37	3.88
	protein heterodimerization activity	GO:0046982	114	11.95
	ligase activity, forming carbon-nitrogen bonds	GO:0016879	35	3.67
	acetylglucosaminyltransferase activity	GO:0008375	35	3.67
oxidoreductase activity	GO:0016638	12	1.26	

3